JOURNAL OF MATERIALS SCIENCE 28 (1993) 4279–4287

Creep of silicon nitride–titanium nitride composites

YU. G. GOGOTSI*, G. GRATHWOHL
Institut für Keramik im Maschinenbau, Universität Karlsruhe, W-7500 Karlsruhe 1, Germany

The effect of particulate TiN additions (0–50 wt%) on creep behaviour of hot-pressed (5 wt% Y_2O_3 + 2 wt% Al_2O_3)-doped silicon nitride (HPSN)-based ceramics was studied. Creep was measured using a four-point bending fixture in air at 1100–1340 °C. At 1100 °C, very low creep rates of HPSN with 0–30 wt% TiN are observed at nominal stresses up to 160 MPa. At 1200 °C the creep rate is slightly higher, and at 1300 °C the creep rate is increased by three orders of magnitude compared to 1100 °C and rupture occurs after a few hours under creep conditions. It was established that the formation of a TiN skeleton could detrimentally affect the creep behaviour of HPSN. An increase in TiN content leads to higher creep rates and to shorter rupture times of the samples. Activation energies of 500–1000 kJ mol^{-1} in the temperature range of 1100–1340 °C at 100 MPa, and stress exponents $n \leqslant 4$ in the stress range 100–160 MPa at 1130–1200 °C were calculated. Possible creep mechanisms and the effect of oxidation on creep are discussed.

1. Introduction

The application of ceramics as high-temperature materials is proposed for many purposes, e.g. in engines and energy systems. In order to replace metals for application under these severe conditions, outstanding properties are required for ceramics to be considered as alternative materials to superalloys. In the high-temperature regime, the highest strength values for structural ceramics are offered by the various Si_3N_4 materials. Therefore, the creep of traditional reaction-sintered and hot-pressed Si_3N_4 (HPSN)-based materials has been investigated quite thoroughly [1–4]. Various mechanisms have been suggested to explain the creep of glass-containing ceramics such as sintered or hot-pressed silicon nitride. These include dissolution–reprecipitation creep, dissolution-enhanced plasticity, and viscous flow [5], but Si_3N_4-matrix composites have not been studied so well. Recently, increased attention has been devoted to particulate additions for the production of structural Si_3N_4-based ceramics [6, 7]. SiC [6], TiC[7, 8] or TiN [9–18] are most frequently used for particulate reinforcement of the silicon nitride matrix. The thermal expansion mismatch between added particles and Si_3N_4 matrix will produce compression stresses in the matrix during cooling after the composite is sintered at high temperature. The introduction of TiN particles into a silicon nitride matrix can increase its fracture toughness, wear resistance and Young's modulus [10, 12]. This makes possible electro-discharge machining of the ceramics and their use for some specific applications, such as heaters, commutators, collector rings, etc. [11]. The alteration of the Si_3N_4 microstructure by the dispersed additions may then offer a potential for improvement of the composite's strength at room temperature but the effect at elevated temperature may be adverse [8]. In particle-strengthened metallic alloys, values of the stress exponent and activation energy for creep which are larger than those measured for single-phase materials have been observed [19].

In the earlier work on silicon nitride and sialons, it has been also demonstrated that oxidation may have a profound influence on the microstructure of these materials by modification of the intergranular phase [1, 2]. This phase plays a crucial role in the creep behaviour of these materials: in order to reach the highest creep resistance, amorphous or glassy phases have to be minimized at grain boundaries and triple-grain junctions. Hence creep tests in oxidizing, or more generally corrosive environments, may give rise to rather complex effects, because the microstructure of the material is not in a stationary state.

The main objective of this paper is to report some new results emanating from studies carried out on Si_3N_4 materials with different content of TiN in a high-temperature oxidizing environment. Creep measurements were performed with the aim to evaluate the effects of the content of particulate TiN additions and the environment on high-temperature properties of silicon nitride-based ceramics.

2. Materials

The materials tested in this study included samples of hot-pressed silicon nitride with different amounts of TiN (Table I) developed at the Institute for Problems of Materials Science, Kiev, Ukraine. The mixtures were prepared by milling of Si_3N_4 with oxide additives (5 wt % Y_2O_3 and 2 wt % Al_2O_3) and TiN powder in

* Present address: Tokyo Institute of Technology, Research Laboratory of Engineering Materials, 4259 Nagatsuta, Midori-ku, Yokohama 227, Japan.

0022–2461

TABLE I Characterization of materials

Material	TiN content (wt %)	Density ($g\,cm^{-3}$)	Young's modulus (GPa)	K^a_{1c} (MPa $m^{1/2}$)	HV[a] (GPa)
HPSN	0	3.29	290	7.5	15.03
HPSN–10TiN	10	3.31	303	8.5	15.24
HPSN–30TiN	30	3.60	324	8.9	16.05
HPSN–40TiN	40	3.78	334	8.9	14.49
HPSN–50TiN	50	3.96	350	9.1	14.86

[a] Vickers indentation with 49 N.

TABLE II Composition of materials

Material	Elements (wt %)						
	Y	Al	Ti	W	Co	Si	N
HPSN–10TiN	3.05	1.26	7.70	0.91	0.13	53.48	33.57
HPSN–30TiN	2.40	1.23	20.70	1.50	0.21	40.82	33.14
HPSN–40TiN	1.84	1.11	27.40	1.50	0.19	35.05	32.91
HPSN–50TiN	1.47	0.86	29.87	0.91	0.15	27.16	39.58

a ball mill for obtaining a uniform distribution of TiN particles in sintered bodies. The median grain size of TiN particles after milling was < 1 μm [12]. The composition of ceramics after hot pressing is described in Table II.

The hot pressing of samples was performed in graphite moulds without an inert atmosphere. From the obtained plates (6 mm × 50 mm × 50 mm), the test samples (of dimensions 3.5 mm × 4.5 mm × 45 mm) were cut.

The structure and properties of baseline TiN-free ceramics with the same composition (Si_3N_4 + 5 wt % Y_2O_3 + 2 wt % Al_2O_3) are described by Gogotsi *et al.* [13]. The studies of the microstructure of TiN-containing ceramics (Fig. 1) demonstrated that TiN grains are relatively uniformly distributed in the silicon nitride matrix (at < 30 wt % TiN) or form a continuous skeleton (at 40–50 wt % TiN), which has been proved by the results of electroconductivity measurements [12]. The investigation of fracture surfaces revealed that the average grain size of the silicon nitride matrix was < 1 μm, the composition of the matrix being rather non-uniform and including β-Si_3N_4, WSi_2, and traces of $Y_{10}Al_2Si_3O_{18}N_4$, $Y_5(SiO_4)_3N$ and $YSiO_2N$. The grain size of β-Si_3N_4 decreased slightly with increasing TiN content (Fig. 1). The transmission electron microscopy (TEM) investigations showed the presence of a glassy or partially crystalline intergranular phase in the triple-point junctions. The starting materials were primarily dislocation free. Inclusions were found in some large β-Si_3N_4 grains. Some physico-mechanical properties and the oxidation behaviour of these materials were described earlier [12–14].

3. Experimental procedure

Creep was measured using a four-point bending fixture with the distances between the inner and outer loading points being 20 and 40 mm, respectively. The

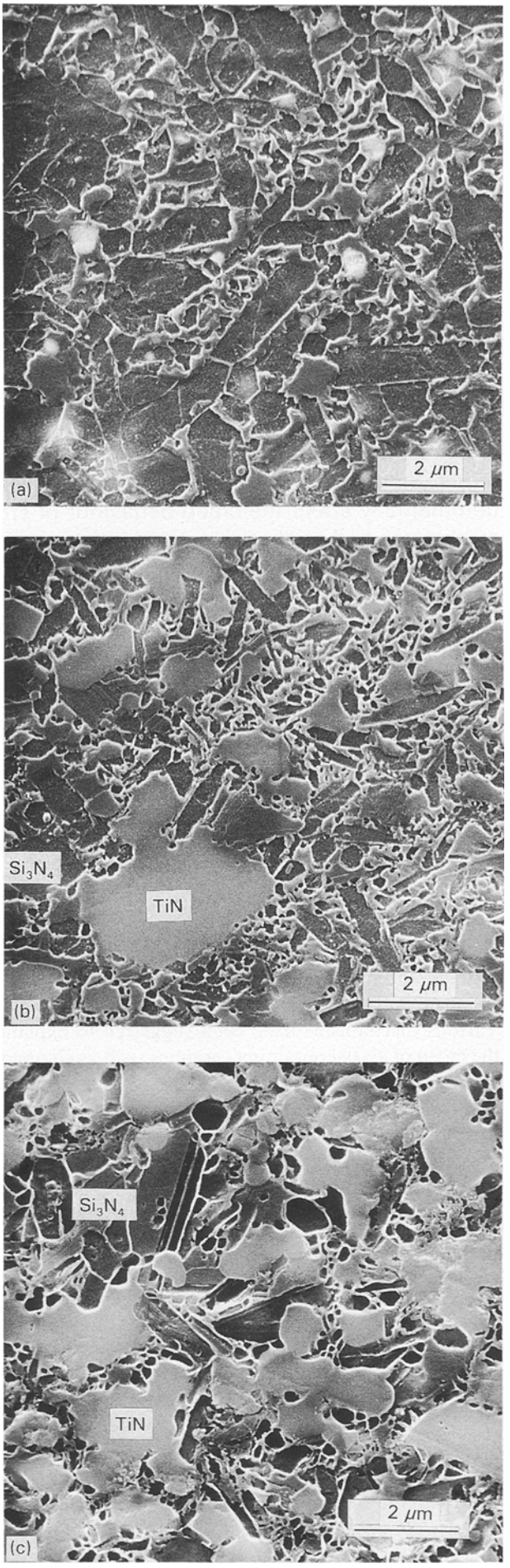

Figure 1 Scanning electron micrographs of polished and plasma-etched surfaces of (a) HPSN, (b) HPSN–30TiN and (c) HPSN–50TiN.

creep tests were performed in air at temperatures between 1100 and 1340 °C in the stress range of 100–160 MPa. To evaluate the temperature range of softening of ceramics, some experiments were carried out under stress of 100 MPa and heating rate of 10 °C min^{-1} from room temperature until failure of the specimen. All components of the fixture which were in contact with a sample were made from sintered SiC. The sample deformation was measured continuously as midpoint deflection on the tension surface. Linear variable transducers with a sensitivity of about 0.1 mmV^{-1} were used. Stress and strain were calculated using elastic beam equations.

Oxidation of the specimens in air under programmed heating up to 1500 °C was studied using a Netzsch thermobalance capable of 20 μg resolution. Three-point bending tests (with a span of 20 mm) were made in vacuum in the temperature range 20–1500 °C.

Samples before and after creep experiments were examined by X-ray diffraction (Siemens, D500), TEM (Hitachi 200 kV), SEM (International Scientific Instruments, ISI-60 and Jeol, Superprobe 733) and metallography (Zeiss, Axiomat). TEM sections were taken from the gauge section. Microstructural analyses were conducted on specimens that failed during creep and on specimens from tests that were interrupted before fracture. The latter were cooled under load to prevent stress relaxation.

Scanning acoustic microscopy (Leica, ELSAM) and scanning laser acoustic microscopy were used to detect the subsurface flaws in ceramic samples after creep tests.

4. Results and discussion

4.1. Effect of particulate additives

The observations of the temperature dependence of three-point bending strength are shown in Fig. 2a. In all instances the strength decreases above 1000 °C. The strain diagrams obtained under the constant stress of 100 MPa and the heating rate of 10 °C min^{-1} are presented in Fig. 2b. This figure shows that the sharp strain increase occurs for ceramics with a higher TiN content at lower temperatures.

As can be seen in Fig. 3, a very low creep rate is observed for HPSN at a nominal stress of 100 MPa at 1100 °C. At 1200 °C, the creep rate is only slightly higher, but at 1300 °C it exceeds the rate at 1100 °C by three orders of magnitude (Fig. 3a) and rupture of the specimens is observed after a few hours under creep stress. At relatively low stresses and temperatures the deformation kinetics remain in an apparently steady state for all material combinations and the tertiary stage with an acceleration of the creep rate is only observed at the highest temperatures. The sharp increase of the creep rates and the decrease of the times to rupture of HPSN observed in the temperature range 1250–1300 °C may be the result of a change in the rupture regime, i.e. from slow crack growth to creep-controlled rupture [20].

An important characteristic of the ceramics under study is the occurrence of transient creep for all compositions during a very long period of time. This

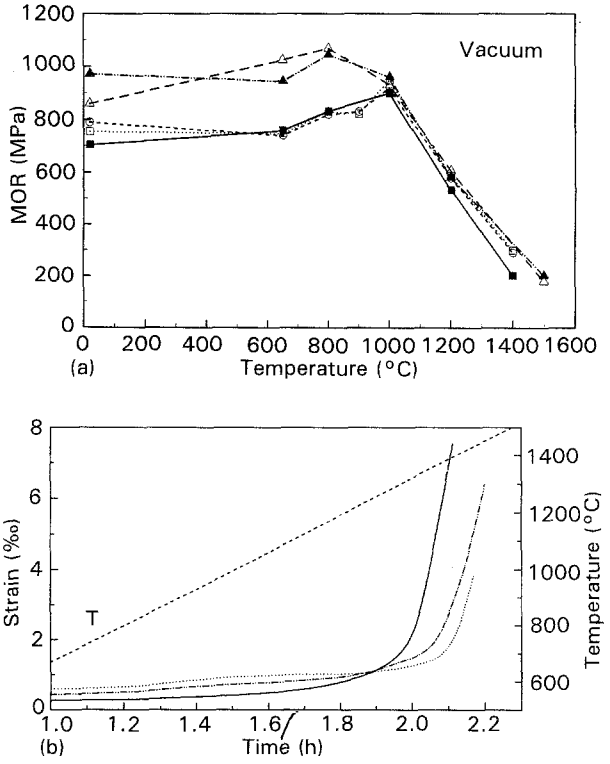

Figure 2 Temperature effect on (a) strength and (b) strain–temperature diagrams, for ceramics with different TiN contents. (a) Vacuum, (○) HPSN, (□) HPSN–10TiN, (△) HPSN–30TiN, (▲) HPSN–40TiN, (■) HPSN–50TiN. (b) Heating rate 10 °C min^{-1}, 100 MPa, (· · ·) HPSN, (— · —) HPSN–10TiN, (——) HPSN–40TiN.

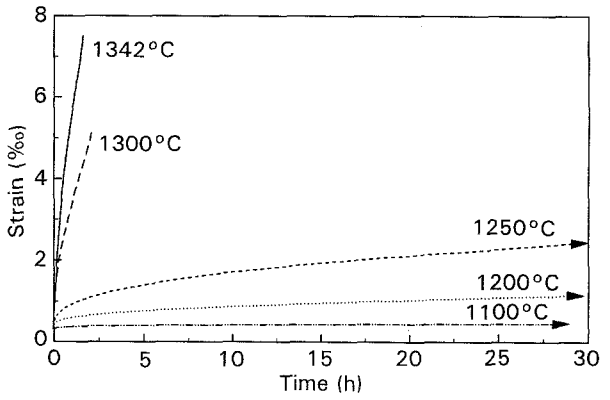

Figure 3 Creep curves of HPSN at different temperatures, at 100 MPa.

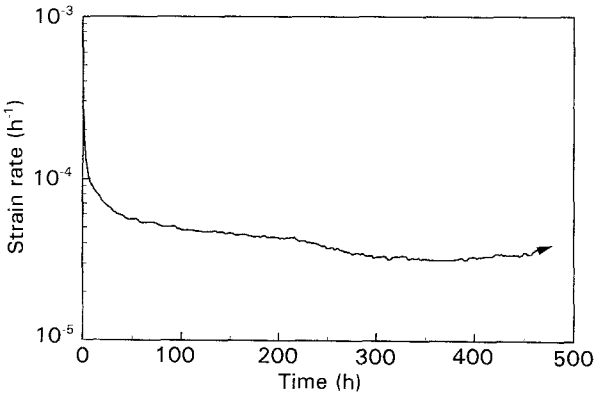

Figure 4 Creep curve of an HPSN–40TiN sample tested at 1200 °C, 100 MPa.

behaviour is illustrated in Fig. 4 for a specimen with 40 wt % TiN. As can be seen, the creep rate continuously decreases as a function of time. Only after 300 h the creep rate seems to reach an apparently steady state stage.

This transient behaviour may be attributed to:

(i) viscous flow of glass between the grains and transfer of load from the glassy intergranular phase to the grains;

(ii) devitrification of intergranular phases;

(iii) changes of the composition of the intergranular phase due to oxidation and grain-boundary diffusion.

As can be seen in Fig. 5, the increase of TiN content in ceramics leads to higher creep rates, macroscopic deformation and shorter rupture times of the samples. It must be recognized that the effect of TiN additions on the creep rate is observed over the whole temperature range studied. In contrast, short-term bending strength of these ceramics above 1100 °C in vacuum is almost independent of the TiN content (Fig. 2a). Only for HPSN–50TiN were somewhat lower strength values measured.

It should be noted that the total content of oxide additives in ceramics decreases with the increase of the TiN content (Table II). For ceramics with a lower content of intergranular phase, lower creep rates are usually observed. The inverse dependence found for the materials under study may be the result of a very strong effect of TiN on the creep rates. On the other hand, the interaction of TiO_2, which is always present on the surface of TiN particles, with Si_3N_4 during hot pressing according to the reaction [18]

$$6\,TiO_2 + 2\,Si_3N_4 = 6\,TiN + 6\,SiO_2 + N_2 \quad (1)$$

can change the composition of the intergranular phase and affect its properties.

The minimum creep rates of all materials tested at 100 MPa are summarized in Fig. 6 as a function of the TiN content. As can be seen, the addition of up to 30 wt % TiN leads only to a slight increase in the creep rate. A sharp increase in the creep rates (Fig. 6) and shorter lifetimes (Fig. 5) are observed for specimens with a higher TiN content. Probably, the formation of a TiN skeleton detrimentally affects the creep behaviour of HPSN. Fine-grained matrix microstructure (Fig. 1) in the ceramics with higher TiN contents can also be responsible for the increase of the creep rate as compared to the Si_3N_4 ceramic.

It was proposed [16] that the dependence of the creep rates of composites, $\dot{\varepsilon}$, on the TiN content can be described by an empirical law of the form

$$\dot{\varepsilon} = \dot{\varepsilon}_0(1 + (V/d)k) \quad (2)$$

where $\dot{\varepsilon}_0$ is the creep rate of the matrix, V/d the volume fraction/particle size ratio, and k a constant depending on the temperature. The results of the Fig. 6 however, contradict Equation 2; a non-linear dependence of the creep rate on the TiN content was found. A close to exponential dependence of the creep rate on the TiN content is observed at intermediate temperatures (1200–1250 °C) and a stronger change is manifested at > 30 wt % TiN at all temperatures applied in the tests. This result suggests that creep of these materials is controlled by at least two different mechanisms depending on TiN content and temperature.

The heavy oxidation of virgin fracture surfaces generated during creep tests (Fig. 7) makes any fractography and detection of fracture origins difficult. However, the macroscopic differences in the morphologies of the fracture surfaces can clearly be observed (Fig. 8). All fractographs show the occurrence of subcritical crack growth (SCG). Optical micrographs of the fracture surfaces reveal different features depending on the TiN content; the fracture surfaces

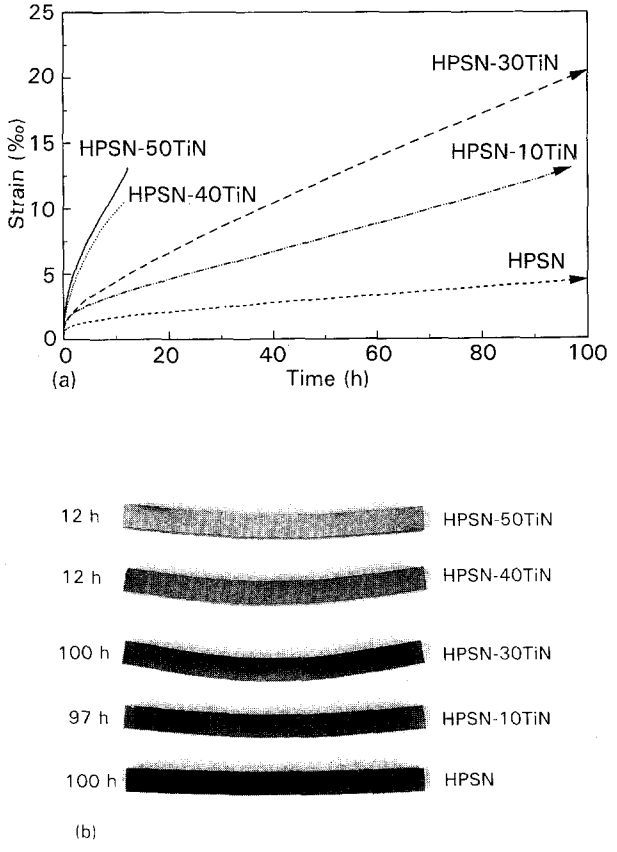

Figure 5 (a) Creep curves of ceramics with different TiN contents at 1250 °C, and 100 MPa, (b) the appearance of the specimens after the tests.

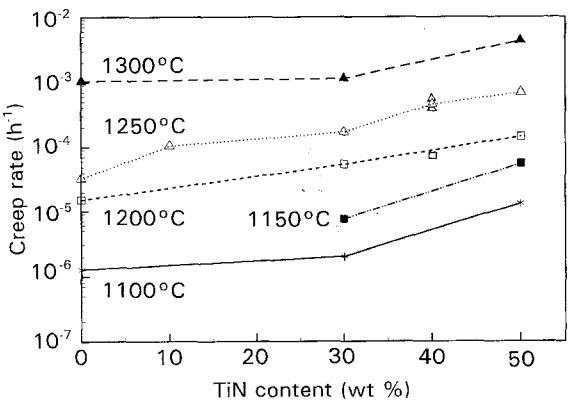

Figure 6 Dependence of the minimum creep rate at different temperatures on the TiN content in Si_3N_4 ceramics.

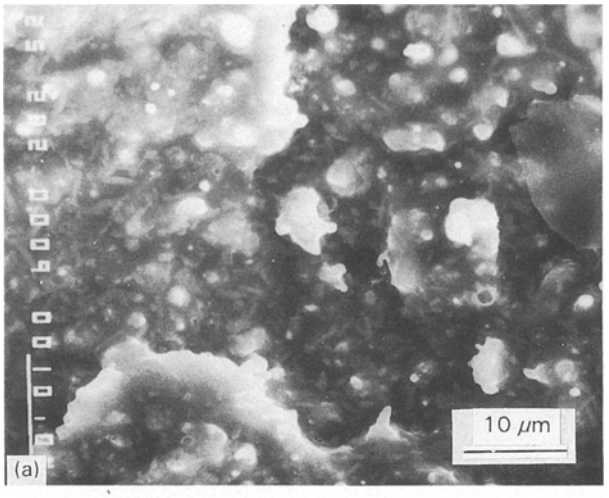

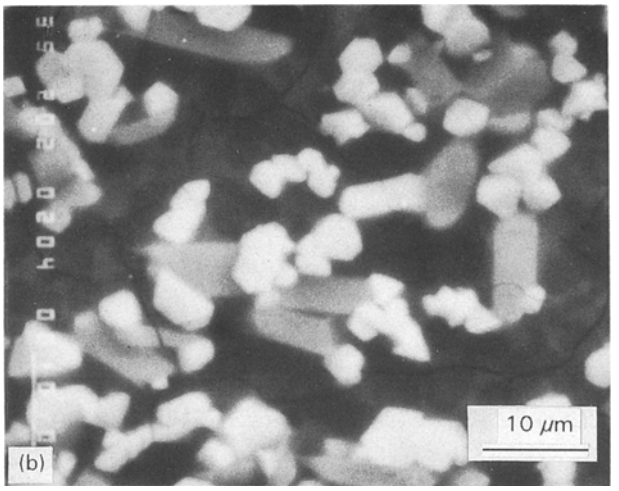

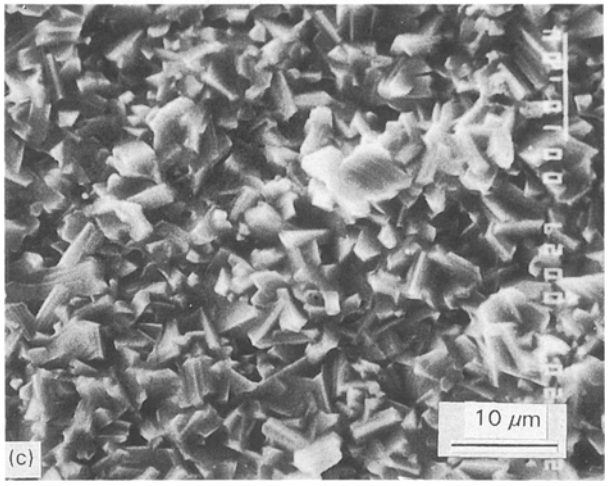

Figure 7 Scanning electron micrographs of fracture surfaces of (a) HPSN, (b) HPSN–30TiN and (c) HPSN–50TiN samples failed at 1300 °C.

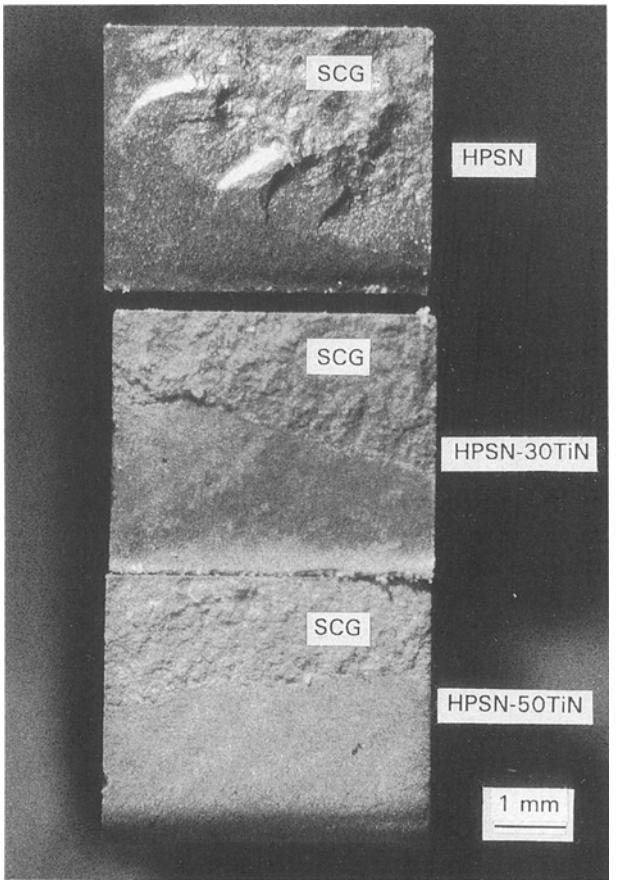

Figure 8 General view of the fracture surfaces of HPSN, HPSN–30TiN and HPSN–50TiN samples failed at 1300 °C.

appear generally smoother with increasing TiN content.

It is important to notice that the various methods of non-destructive testing, as well as the SEM investigations of the creep specimens, did not reveal any surface cracking in the samples tested below 1250 °C. Cracks were found only in ceramics with ≤ 30 wt % TiN at higher temperatures and loading times of about 100 h (Fig. 9). The cracks were sealed by a silicate film which probably protects the specimen against inner oxidation (Fig. 9a, c).

Owing to the transient creep behaviour the effect of temperature and stress on creep was studied using the minimum creep rate. The dependence of the secondary creep rate, $\dot{\varepsilon}$, on stress, σ, can be described by the equation

$$\dot{\varepsilon} = A\sigma^n \quad (3)$$

The stress exponent, n, was determined by stress change experiments for stress changes 100–130–160 MPa at 1100–1200 °C (Fig. 10a). n was found to be of the order of 1 for HPSN (Table III). A sharp increase of n was observed for ceramics with 10 wt % TiN and a decrease of n with further increase of TiN content. A very weak dependence of the creep rate on the applied stress and $n < 1$ for ceramics with the maximum TiN content can be explained by a profound effect of oxidation on creep of this ceramic, which will be discussed later.

From the Arrhenius equation

$$\dot{\varepsilon} = A\exp(-Q/RT) \quad (4)$$

activation energies, Q, at temperatures between 1100 and 1340 °C were found to be in the range 488–1000 kJ mol^{-1} with some decrease to higher TiN content (Table IV, Fig. 10b). These values are in agreement with the results obtained for HPSN in the

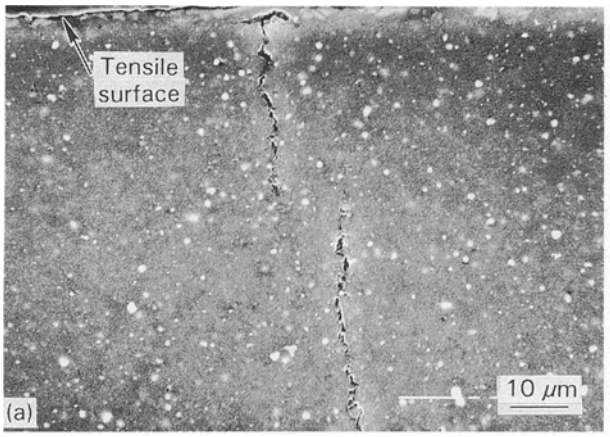

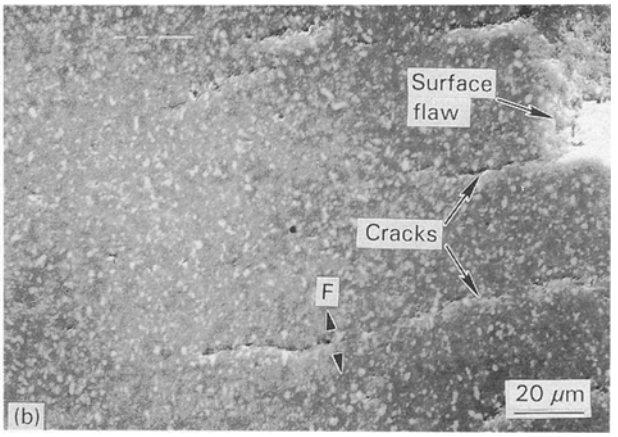

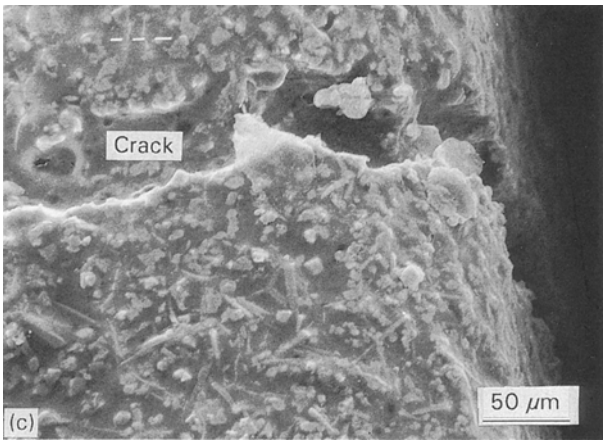

Figure 9 Cross-sections of (a) the HPSN sample tested at 1300 °C and (b) the HPSN–30TiN sample tested at 1250 °C, and (c) the surface of the same HPSN–30TiN sample (stress 100 MPa, time 100 h).

TABLE III Stress exponents from Equation 3 for stress changes 100–130–160 MPa

Material	Temperature (°C)	Stress exponent, n
HPSN	1200	1.3
HPSN–10TiN	1200	4.1
HPSN–30TiN	1200	2.6
HPSN–30TiN	1130	1.8
HPSN–40TiN	1100	1.7
HPSN–50TiN	1155	0.5

TABLE IV Activation energies calculated from Equation 4 for creep under a nominal stress of 100 MPa

Material	Temperature range (°C)	Apparent activation energy (kJ mol^{-1})
HPSN	1100–1250	384
HPSN	1250–1340	1000
HPSN–10TiN	1200–1250	636
HPSN–30TiN	1100–1300	562
HPSN–40TiN	1100–1250	488
HPSN–50TiN	1100–1300	509

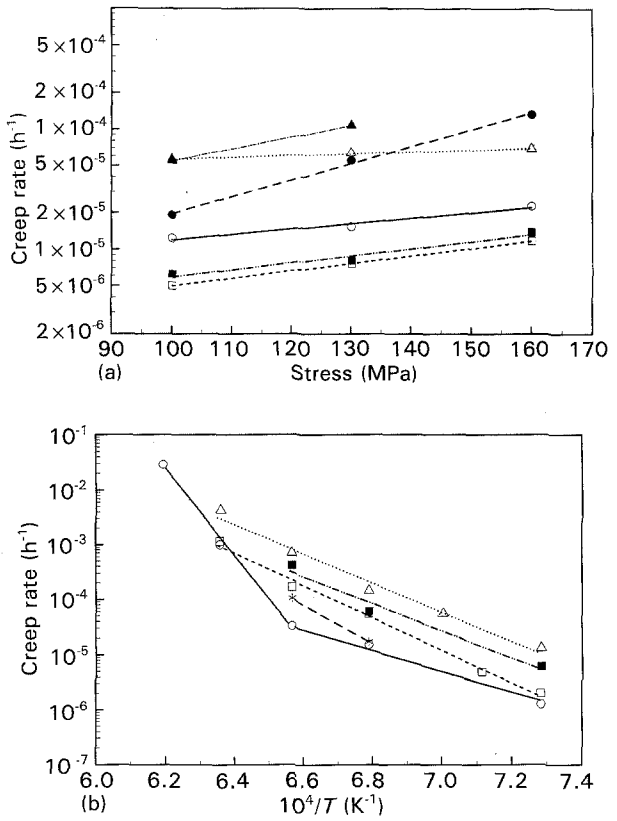

Figure 10 Dependencies of the creep rates on (a) stress and (b) reciprocal temperature for ceramics with different TiN contents at 100 MPa. (a) (○) HPSN, (●) HPSN–10TiN, (□) HPSN–30TiN (1130 °C), (▲) HPSN–30TiN (1200 °C), (■) HPSN–40TiN, (△) HPSN–50TiN. (b) (○) HPSN, (*) HPSN–10TiN, (□) HPSN–30TiN, (■) HPSN–40TiN, (△) HPSN–50TiN.

same temperature range [20] and with values obtained for Si_3N_4–40 vol % TiN composites from compression creep tests [8]. The slight bend on the Arrhenius plot for the HPSN and the higher values of the activation energy at 1250–1340 °C indicate that a change of the deformation mechanism occurs. It was shown previously [20] that for HPSN at high temperatures a characteristic stress exists which allows a clear distinction between the materials response at the low- and the high-stress level. In the low-stress region, the time to failure is strain controlled and the kinetics of stress rupture can straightforwardly be analysed using conventional creep equations. At higher stresses, subcritical growth of pre-existing flaws is suggested to control the rupture behaviour of ceramics. This stress limit is temperature dependent. Probably, the applied

stress of 100 MPa is higher than the critical stress level above 1250 °C and the criterion for failure changes, the rupture behaviour ceases to interfere with the creep strain. The absence of such changes of the creep behaviour for the other ceramics under study relates to the presence of TiN. In this regard, TiN additive has a profound effect on the process of deformation during flexure creep tests.

The effect of TiN additions on the deformation characteristics of HPSN can be considered on the basis that the creep rate of the matrix is controlled primarily by solution–diffusion–precipitation processes which accommodate grain-boundary sliding. By incorporating the TiN particles, the interface-boundary sliding can no longer be accommodated by such material transport to preserve the integrity of the material, and cavities in the deformed samples were observed to grow predominantly into the interface boundaries [15, 16]. Owing to the thermal expansion mismatch between the particles and the silicon nitride matrix, additional stresses could arise along the phase boundaries and they were found [15] to be then the primary sites of cavity nucleation and propagation. However, this observation contradicts the low values of the stress exponent measured for ceramics with high TiN contents by compression and bending tests. High values of the stress exponent (4–13.5 [3, 4]) are usually observed when cavitation accompanies creep. n values of ~ 4 were found in our experiments only for ceramics with 10 % TiN. An easy formation of cavities along the grain boundaries was observed also for Si–SiC and Si_3N_4–SiC composites [21]. Cavities were always located at Si/SiC or Si_3N_4/SiC interfaces, most often between the closely spaced SiC grains. Once nucleated, the cavities in these ceramics tend to grow completely across the facet forming a microcrack, which then acts as a stress concentrator, assisting in the formation of cavities along the interfaces of adjacent grains, thus forming a self-propagating crack that eventually results in failure.

In our investigations, very few macrocracks such as that shown in Fig. 9 were observed in the cross-section of the specimens that have been crept to failure, suggesting that once formed, these large cracks propagate to failure by subcritical crack growth.

Some strain whorls and numerous intergranular voids and cavities were found along grain boundaries (Fig. 11). They were the manifestation of viscous grain-boundary sliding. But the cavities were not preferably formed along Si_3N_4/TiN boundaries. Most of them were found between Si_3N_4 grains and at the multi-grain junctions (Fig. 11a,d). Once the cavity nucleates, pocket depletion proceeds by viscous flow of the grain-boundary phase into the neighbouring two-grain channels until pocket depletion is completed. Depletion of multigrain junctions can result in various geometries depending on the original junction shape. Usually, triangular shape cavities were found (Fig. 11a,d). These observations are consistent with the presence of high stress exponents with $n \approx 4$ (for ceramics with 10 % TiN). The presence of twins (Fig. 11a) and dislocation networks in TiN grains (Fig. 11c)

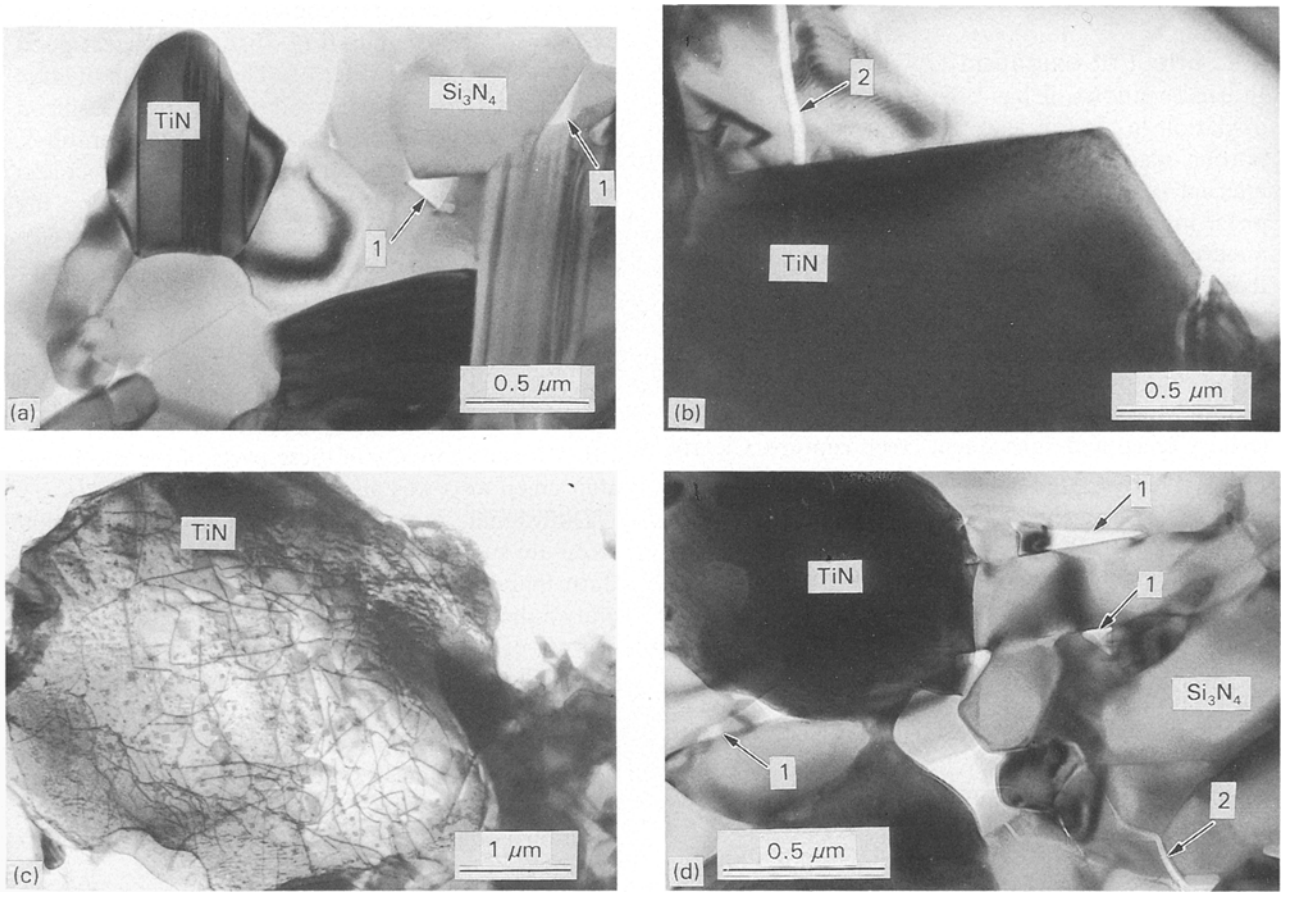

Figure 11 Transmission electron micrographs of (a–c) HPSN–30TiN and (d) HPSN–40TiN samples after creep tests at 1250 °C and 100 MPa during (a–c) 100 h and (d) 12 h. 1, triangular shape cavities; 2, intergranular microcracks.

indicates that the creep of the Si_3N_4 matrix is well accommodated by deformation of TiN particles.

Under these conditions, the steady-state creep rate of the composite material under the applied stress, σ, can be regarded to be controlled by two creep components, being related to the viscous creep or cavitational accommodation of the matrix, and to the plastic deformation of the TiN skeleton. Sometimes the crack-like cavities stop at the TiN grain boundary (Fig. 11b). Numerous twins and dislocations were found in TiN grains after creep tests. A higher dislocation activity was observed for samples with the highest TiN content. The differences in the mechanisms of crack nucleation and growth in pure silicon nitride and composites may be a reason for the different appearances of fracture surfaces (Fig. 8) of TiN-containing and TiN-free ceramics.

Thus, our results of flexure creep tests can give a supplement to the data obtained previously by compression tests [8, 15, 16]. On the one hand the creep rates increased and, on the other hand, the rupture times and fracture stresses decreased, with respect to the matrix, at high TiN contents. However, the investigation of compositions with lower TiN contents shows that these ceramics have a good creep resistance up to 1250 °C and 100 MPa and only slightly increased creep rates compared to TiN-free HPSN are observed. In contrast to the present results, a lower creep ductility was observed for TiN-containing ceramics in compression tests [16]. The elucidation of the reasons for these apparent contradictions require future research.

4.2. Effect of oxidation

In earlier studies, it has been demonstrated [1] that oxidation in air can lead to enhanced creep rates of porous reaction-bonded silicon nitride, because of internal oxidation and formation of viscous glassy phase in the volume of ceramics. Dense silicon nitride materials show lower steady state creep rates in air than in vacuum because of the removal of impurities from the bulk material to the oxide scale. This results in a reduction of the viscosity of the intergranular phase. On the other hand, the degradation of the surface layer due to oxidation can lead to enhanced tertiary creep and subsequent creep rupture. Clearly, surface oxidation occurs in Si_3N_4–TiN ceramics, resulting in composition changes in the subsurface layer during high temperature tests.

The detectable mass gain of TiN-containing Si_3N_4 ceramics starts at > 700 °C (Fig. 12) and up to ~ 900 °C the oxidation rate is very low. When the sample of HPSN–50TiN is heated above 1000 °C, the mass gain increases rapidly and then the rate of mass gain hardly changes up to 1500 °C. For ceramics with ≤ 30 wt % TiN, relatively low oxidation rates were detected up to 1450 °C. under non-isothermal conditions, mass gain was not detected below 1150 °C for baseline HPSN (Fig. 12). It was shown [14] that the mass gain of the composites is controlled predominantly by the oxidation of TiN.

Higher oxidation rates of TiN-containing ceramics

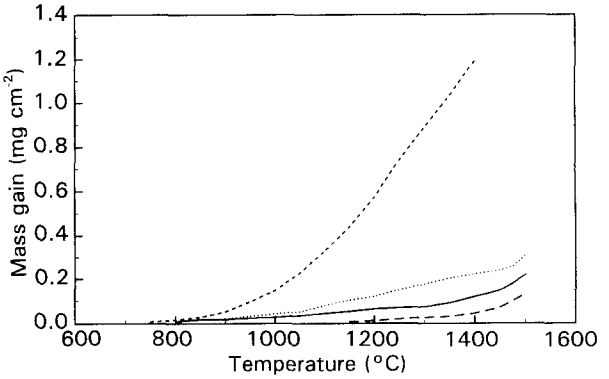

Figure 12 Thermogravimetric curves. Heating rate 10 °C min^{-1}, (– – –) HPSN–50TiN, (· · ·) HPSN–30TiN, (——) HPSN–10TiN, (— — —) HPSN.

(Fig. 12) can be one of the reasons for their lower time to rupture and higher creep rates. The structure of the oxidized surface layer is one of the most important factors which affects the high-temperature performance of materials. As can be seen in Fig. 7, oxidation of all ceramics occurred under test conditions. Up to 1340 °C the surface of HPSN samples is covered by a very thin silicate layer (Fig. 7a). On the surface of the HPSN sample tested during 100 h at 1250 °C, even the grooves from machining can still be clearly seen. The surface of ceramics with 40 or 50 wt % TiN was covered by a thick rutile scale (Fig. 7c) having low protective properties. It has been shown [14] that in this case the oxidation interface can penetrate relatively deeply into the material. The oxide layer on ceramics with lower TiN contents contains inclusions of TiO_2 in a silicate film (Fig. 7b) and possesses good protective properties (Fig. 12). The formation of large surface flaws occurs, as a result of oxidation, in silicon nitride-based ceramics at rather low temperatures, and may be responsible for their fracture. Microcracks can nucleate and propagate from these flaws on the tensile surface, as can be seen in Fig. 9a.

At the same time, applied tensile stresses seem to promote pit formation during oxidation of ceramics under load. Investigations of the polished tensile surfaces of HPSN samples tested at 1200 and 1300 °C showed that large oxidation pits were formed only on the parts of the surface under the highest stress (Fig. 13). A higher porosity of these parts of the specimens after creep tests was also observed.

Diffusional creep and solution–reprecipitation creep are suggested as creep-controlling mechanisms. Both these mechanisms lead to a stress exponent of unity if the kinetics of Fick's law is obeyed [22]. In the process of diffusional creep, self-diffusion within the grains allows the ceramic to yield to an applied stress. Deformation results from diffusional flow within each grain away from the boundaries under compressive stress (high chemical potential) toward boundaries having a zero or tensile stress. For example, a tensile stress on a boundary increases the vacancy concentration to

$$c = c_0 \exp(\sigma\Omega/kT) \quad (5)$$

where Ω is the vacancy volume, and c_0 is the equilib-

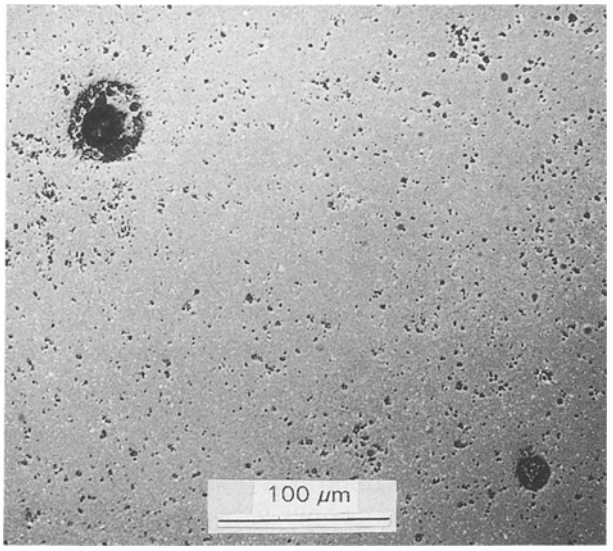

Figure 13 Optical micrograph of the polished tensile surface of the HPSN sample tested at 1200 °C and 160 MPa, showing large oxidation pits and the high porosity of the tensile surface.

rium concentration. During the oxidation of Si_3N_4–TiN composites, diffusion of titanium ions to the reaction interface takes place. The outward diffusion of titanium leads to a high concentration of vacancies in the subsurface layer. Together with the effect of the applied tensile stress, this process helps to accommodate creep deformation on the compression surface and can obviously increase diffusional creep rate in tension. Because a deep penetration of the reaction boundary into the material is possible only for ceramics with > 30 wt % TiN [14], only for these materials with 40 and 50 wt % TiN, were significantly higher creep rates observed (Fig. 6).

5. Conclusions

Flexural creep experiments were performed between 1100 and 1340 °C on hot-pressed ceramics based on silicon nitride. The following results and conclusions were obtained.

1. Creep rate increases and time to rupture decreases with the increase in TiN content in ceramics.

2. The presence of fine isolated TiN particles in the silicon nitride matrix ($\leq$ 30 wt % TiN) only slightly increases the creep rate.

3. For materials containing a continuous TiN skeleton (40–50 wt % TiN) considerably higher creep rates are measured.

4. Creep analysis results in activation energies, Q, ranging from 500–1000 kJ mol^{-1} and increasing with higher TiN content. Stress exponents $n \leq 4$ in the stress range 100–160 MPa were determined.

5. Creep mechanisms in silicon nitride-based composites strongly depend on oxidation processes during the creep tests.

Acknowledgements

The authors thank Dr V. P. Yaroshenko for preparation of the samples, Mr V. V. Kovylyaev for SEM investigations and Mr V. A. Goncharuk for strength measurements (all from the Institute for Problems of Materials Science, Kiev, Ukraine), Dr A. Bellosi, Research Institute for Ceramics Technology, Faenza, Italy, for help with oxidation experiments and enlightening discussions, Professor W. Arnold and Dr U. Netzelmann, Fraunhofer Institute for Non-Destructive Testing, Saarbrücken, Germany, for non-destructive testing of ceramic samples after the creep tests. Y.G. acknowledges the receipt of a Research Fellowship from Alexander von Humboldt Foundation, under which this work was undertaken at the University of Karlsruhe.

References

1. F. THÜMMLER and G. GRATHWOHL, in "MRS International Meeting on Advanced Materials", Vol. 4 edited by M. Doyana, S. Somiya and R. P. H. Chang (Materials Research Society, Pittsburgh, PA, 1989) pp. 237–53.
2. O. VAN DER BIEST, S. VALKIERS, L. GARGUET, P. TAMBUYSER and I. BAELE, *Br. Ceram. Proc.* **39** (1987) 33.
3. M, GÜRTLER and G. GRATHWOHL, in "Proceedings of the 4th International Conference on Creep and Fracture of Engineering Materials and Structures" (Institute of Metals, London, 1989) pp. 399–408.
4. N. J. TIGHE, S. M. WIEDERHORN, T.-J. CHUANG and C. L. McDANIEL, in "Deformation of Ceramic Materials II", edited by R. E. Tressler and R. C. Bradt (Plenum Press, New York, 1984) pp. 587–603.
5. D. S. WILKINSON and M. M. CHADWICK, in "Proceedings of the 11th Risø International Symposium on Metallurgy and Materials Science", edited by J. J. Bentzen J. B. Bilde-Sorensen, N. Christiansen, A. Horsewell and B. Ralph (Risø National Laboratory, Roskilde, 1990) pp. 517–22.
6. R. POMPE, *ibid.*, pp. 97–110.
7. S. T. BULJAN and J. G. BALDONI, *Mater. Sci. Forum* **47** (1989) 249.
8. F. PENI, J. CRAMPON, R. DUCLOS and B. CALES, *J. Eur. Ceram. Soc.* **8** (1991) 311.
9. A. BELLOSI, A. TAMPIERI and YU-ZH. LIU, *Mater. Sci. Eng.* **A127** (1990) 115.
10. A. BELLOSI, S. GUICCIARDI and A. TAMPIERI, *J. Eur. Ceram. Soc.* **9** (1992) 82.
11. Y. YASUTOMI and M. SOBUE, *Ceram. Eng. Sci. Proc.* **11** (1990) 857.
12. V. YAROSHENKO, Yu. GOGOTSI and I. OSIPOVA, in "Ceramics Today—Tomorrow's Ceramics", edited by P. Vincenzini (Elsevier, Amsterdam, 1991) pp. 2821–30.
13. Yu. G. GOGOTSI, O. N. GRIGORJEW and W. P. JAROSCHENKO, *Silikattechnik.* **41** (1990) 156.
14. Yu. G. GOGOTSI and F. PORZ, *Corros. Sci* **33** (1992) 627.
15. J. CRAMPON, R. DUCLOS and P. VIVIER, in "Euro-Ceramics", edited by G. de With, R. A. Terpstra and R. Metselaar (Elsevier, London, 1989) pp. 3.298–3.302.
16. J. CRAMPON and R. DUCLOS, *Acta Metall. Mater.* **38** (1990) 805.
17. C. MARTIN, B. CALES, P. VIVIER and P. MATHIEN, *Mater. Sci. Eng.* **A109** (1989) 351–356.
18. M. HERRMANN, Ch. SCHUBERT, J. PABST, H.-J. RICHTER, P. OBENAUS and V. P. JAROSCHENKO, in "Verstärkung keramischer Werkstoffe", Hamburg, 8–9 October 1991 (Deutsche Gesellschaft für Material-Kunde) to be published.
19. H. E. EVANS, "Mechanisms of Creep Fracture" (Elsevier, London, 1984).
20. G. GRATHWOHL, in "Deformation of Ceramic Materials II", edited by R. E. Tressler and R. C. Bradt (Plenum Press, New York, 1984) pp. 573–86.
21. S. M. WIEDERHORN and B. J. HOCKEY, in "Advanced Structural Inorganic Composites", edited by P. Vincenzini (Elsevier, Amsterdam, 1991) pp. 365–80.
22. C.-F. CHEN and T.-Y. TIEN, *Mater. Sci. Forum* **47** (1989) 204.

Received 24 August 1992
and accepted 3 February 1993